J. Mol. Model. **1998**, *4*, 200 – 210

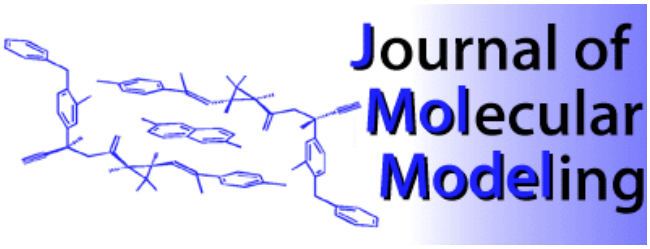

FULL PAPER

Determination of the Solution Conformation of HIV-1 Tat(1-9) Peptides by Means of Molecular Dynamics Simulations Considering NMR Data and Docking Studies into an Active Site Model of DP IV

Annett Fengler[1], Carmen Mrestani-Klaus[1], Dirk Reinhold[2], Sabine Wrenger[2], Siegfried Ansorge[2], Jürgen Faust[1], Klaus Neubert[1], and Wolfgang Brandt[1]

[1]Department of Biochemistry and Biotechnology, Institute of Biochemistry, Martin-Luther-University Halle-Wittenberg, Kurt-Mothes-Strasse 3, D-06120 Halle (Saale), Germany. Tel: +49-345-5524859; Fax: +49-345-5527011.
E-mail: brandt@biochemtech.uni-halle.de

[2]Center for Internal Medicine, Institute of Experimental Internal Medicine, Otto-von-Guericke-University Magdeburg, Leipziger Strasse 44, D-39120 Magdeburg, Germany.

Received: 31 March 1998 / Accepted: 8 June 1998 / Published: 23 June 1998

Abstract The human immunodeficiency virus 1 Tat protein suppresses antigen-, anti-CD3- and mitogen-induced activation of human T cells when added to T cell cultures. This activity is important for the development of AIDS because lymphocytes from HIV-infected individuals exhibit a similar antigen-specific dysfunction. Moreover, Tat was found to interact with dipeptidyl peptidase IV (DP IV). To find out the amino acid sequence important for the inhibition of the DP IV enzymatic activity we investigated N-terminal Tat(1-9) peptide analogues with amino acid substitutions in different positions. Interestingly, the exchange of Pro^6 with Leu and Asp^5 with Ile strongly diminished the DP IV inhibition by Tat(1-9). Based on data derived from one- and two-dimensional ^1H NMR investigations the solution conformations of the three nonapeptides in water were determined by means of molecular dynamics simulations. These conformations were used for studies of the docking behavior of the peptides into a model of the active site of DP IV. The results suggest that several attractive interactions between the native Tat(1-9) and DP IV lead to a stable complex and that the reduced affinity of both L^6-Tat(1-9) and I^5-Tat(1-9) derivatives might be caused by conformational alterations in comparison to the parent peptide.

Keywords HIV-1 Tat, Dipeptidyl Peptidase IV, Molecular dynamics, AMBER

Correspondence to: W. Brandt

Introduction

HIV-1 Tat protein**,** a short protein consisting of 86 amino acids, is a transactivator regulating the transcription of viral genes and is essential for viral replication in vitro. Tat is also responsible for immunosuppression of non-HIV-1 infected T cells found in acquired immunodeficiency syndrome (AIDS) patients [1,2].

Viscidi *et al.* have discovered that Tat has an additional biological activity, it suppresses antigen-induced T cell proliferation of human lymphocytes [3]. This activity is clinically relevant because lymphocytes from HIV-1 infected individuals exhibit a similar antigen-specific defect [1,4].

It was found that Tat binds to the cell surface protein CD26 / DP IV (dipeptidyl peptidase IV) and inhibits its peptidase activity [5,6]. The addition of soluble DP IV restored the defective in vitro recall antigen response, probably by serving as a decoy receptor for HIV-1 Tat what has been shown [7].

Recently obtained results indicate that the N-terminal Tat(1-9) sequence (MDPVDPNIE) is responsible for the inhibition of the enzymatic activity of DP IV [8,9]. In order to elucidate the essential amino acid residues for the interaction with this enzyme, several derivatives of Tat(1-9) have been synthesized and characterized with regard to their inhibitory potency to DP IV. The DP IV catalyzed hydrolysis of interleukin-2 (IL-2(1-12)) was used to measure their inhibitory activity. Details of peptide synthesis and experimental conditions of the DP IV assay are described in [9]. From these studies it appeared that L^6-Tat(1-9) (about 20% inhibition) and I^5-Tat(1-9) (about 10% inhibition) derivatives show considerably reduced affinity to DP IV whereas the P^2-Tat(1-9) (about 60% inhibition) exhibits practically the same inhibition as the parent peptide.

The substrate specificity of DP IV has been well characterized. DP IV is an exopeptidase which cleaves N-terminal dipeptides from oligopeptides with unsubstituted N-termini, if the penultimate amino acid is proline or alanine [10]. DP

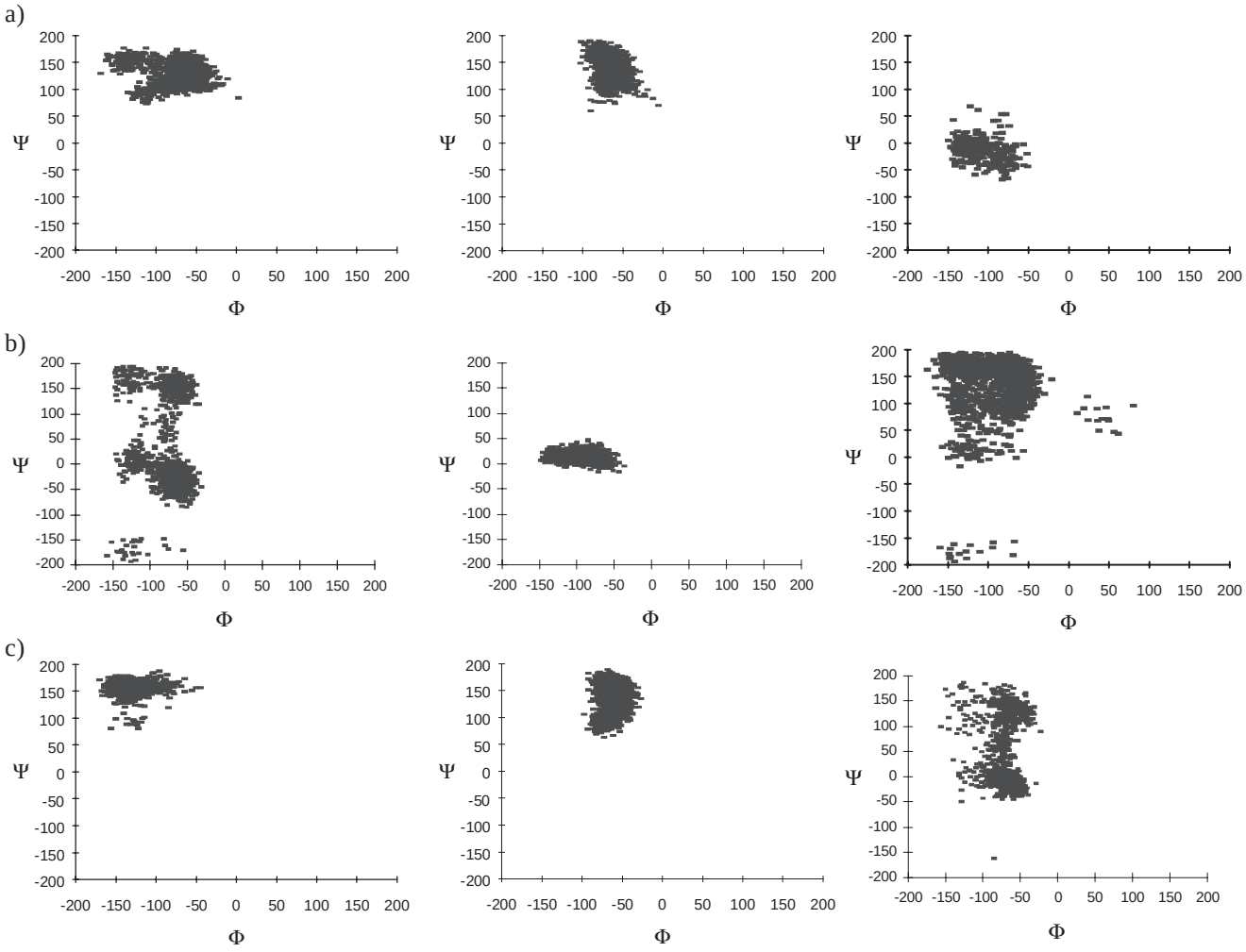

Figure 1 *Plots of the torsion angles Φ and Ψ (°) distribution in the dynamics simulations with distance restraints of a) Tat(1-9), b) L^6-Tat(1-9) and c) I^5-Tat(1-9) of the amino acid residues 5, 6 and 7 (from left to right)*

IV requires a *trans* peptide bond between the P_1 and P_2 residues [11]. If an additional proline is in the third position then these peptides are resistant to cleavage. Some aspects of the substrate specificity of DP IV could be explained by suggesting a substrate recognition conformation which is mainly characterized by a C_7 conformation ($\Psi \sim 80°$) including the proline (or alanine) residue in P_1-position [12]. Up to now no X-ray structure of DP IV or of any related proline specific protease is known. A model of the active site of DP IV was proposed by us on the basis of site directed mutagenesis results and systematic modeling studies including CoMFA [13]. With the help of this model we could explain the proline specificity of DP IV and other unusual experimental findings as well as a quantitative correlation between interaction energies of inhibitors and their pK_i values could be obtained. A recently proposed new mechanism of the serine protease catalysis exhibited by DP IV based on semiempirical studies helps to understand its enzyme action on the molecular level [14]. All these molecular modeling results together should provide sufficient information for the analysis of a possible mechanism of the interaction of Tat(1-9) and its derivatives with the active site model of DP IV.

The biological results of Tat(1-9) interactions with DP IV could not clearly indicate whether Tat(1-9) binds directly at or near to the active site of DP IV and what are the reasons for the reduced inhibitory activity of both the I^5 and L^6 Tat derivatives. These effects may be caused either by conformational alterations in the solution conformation of the Tat derivatives or by different docking behavior to DP IV.

To analyze the first opportunity we performed molecular dynamics simulations based on NMR measurements of all three Tat derivatives. The NMR data in detail will be published elsewhere [15]. The determined conformations which reflect the experimental data best are used for docking studies into the model of the active site of DP IV. The comparison of the docking behavior of the three Tat peptides to the model of the active site of DP IV should help to analyze the most important residues of the ligands for the interactions with DP IV and their differences in inhibitory activities. Based

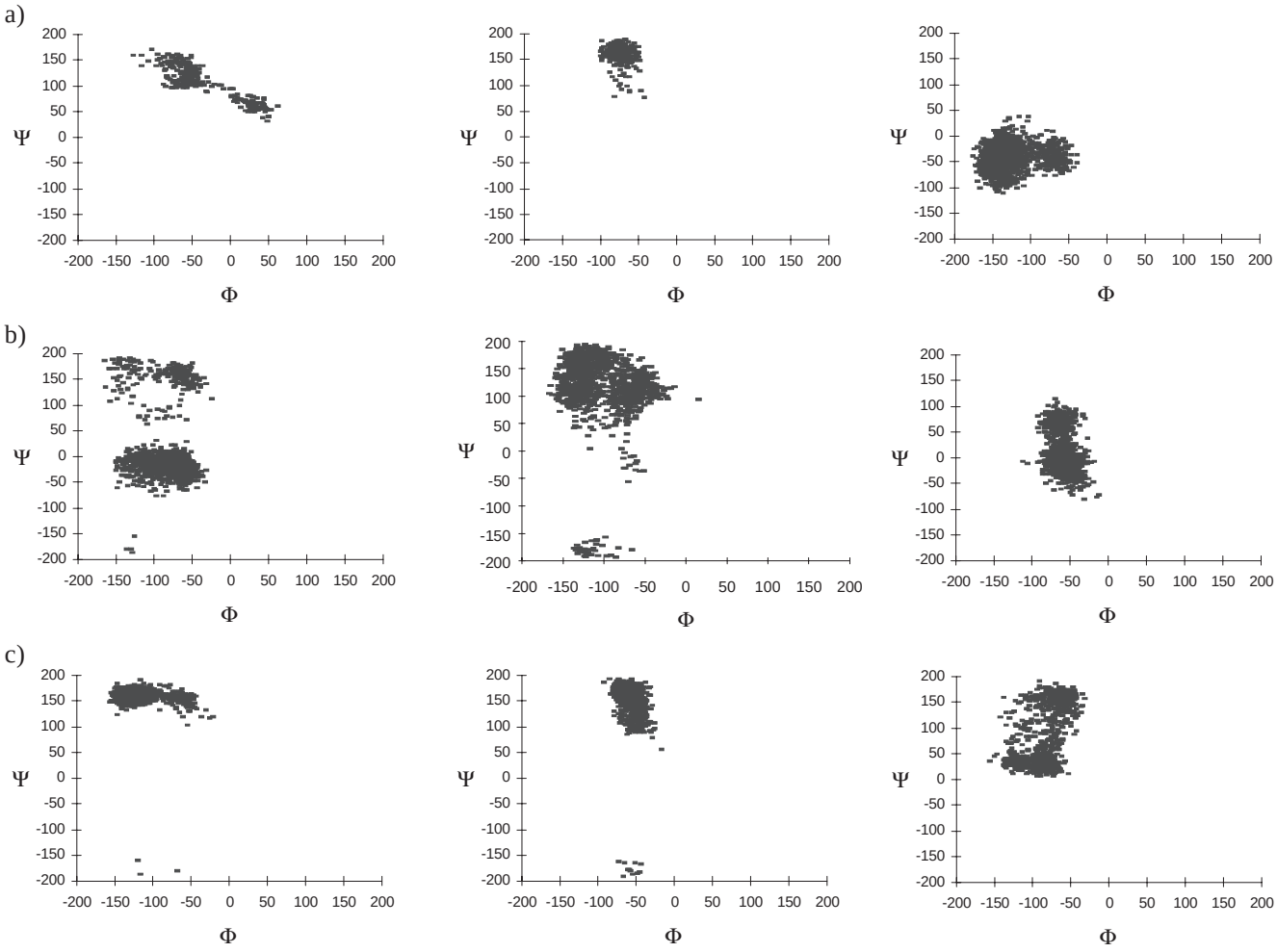

Figure 2 *Plots of the torsion angles Φ and Ψ (°) during the dynamics simulations without distance restraints of a) Tat(1-9), b) L^6-Tat(1-9) and c) I^5-Tat(1-9) of the amino acid residues 5, 6 and 7 (from left to right)*

Table 1 *Dihedral angles (°) of the major solution conformations of Tat(1–9), L^6–Tat(1–9) and I^5–Tat(1–9)*

	torsion angles	Met[1]	Asp[2]	Pro[3]	Val[4]	Xaa[5]	Xaa[6]	Asn[7]	Ile[8]	Glu[9]
Tat(1–9)	$\Phi_{Karplus}$	–	-79	–	-153	-84	–	–153	-149	-88
Xaa[5]=Asp	Φ	–	-70	-54	-142	-66	-75	-138	-151	-86
Xaa[6]=Pro	Ψ	163	163	167	167	146	179	42	165	–
	χ_1	60	-55	-27	-62	55	30	-63	56	-168
	χ_2	175	–	36	–	–	-35	-103	168	-78
	χ_3	-174	–	-31	–	–	29	–	–	–
L^6–Tat(1–9)	$\Phi_{Karplus}$	–	-80	–	-83	-87	-82	-152	-149	-87
Xaa[5]=Asp	Φ	–	-58	-77	-72	-69	-75	-144	-138	-68
Xaa[6]=Leu	Ψ	147	153	164	166	-20	162	155	171	–
	χ_1	-170	58	32	-68	-58	-73	-179	43	62
	χ_2	176	–	-36	–	–	72	-113	62	-175
	χ_3	176	–	28	–	–	–	–	–	–
I^5–Tat(1–9)	$\Phi_{Karplus}$	–	-160	–	-87	-145	–	-82	-149	-153
Xaa[5]=Ile	Φ	–	-139	-75	-79	-139	-58	-64	-133	-138
Xaa[6]=Pro	Ψ	131	100	171	94	163	166	136	116	–
	χ_1	-66	-179	31	-179	57	-24	176	-61	-153
	χ_2	-178	–	-35	–	–	35	-116	176	71
	χ_3	180	–	26	–	–	-33	–	–	–

on these results conclusions for the synthesis of new derivatives will be drawn.

Materials and methods

Molecular modeling studies

The calculations were done using the AMBER 4.1 force field [16,17]. In all cases the N-terminus was positively and the C-terminus was negatively charged. The peptides were constructed in an extended, *all-trans* conformation and subsequently optimized in the gas phase.

The three nonapeptides were immersed on average by 1400 water molecules using a precomputed cubic water box (TIP3P water model).

The initial structures were subjected to molecular dynamics simulations with the inclusion of H,H distance restraints listed in Table 2 derived from the ROESY experiments. The distance restraints were grouped into 1.8 Å to 2.5 Å (strong), 2.5 Å to 3.3 Å (middle) and 3.3 Å to 4.0 Å (weak) in correspondence to the NOEs and were applied with a force constant of 32 kcal·Å^{-1}.

All molecular dynamics simulations were carried out using periodic boundary conditions. The residue-based cutoff distance for nonbonded interactions was set to 10 Å and subjected to energy minimization until an energy gradient less than 0.0005 kcal·mol^{-1}·Å^{-1} was reached. After 20 cycles the method of minimization was changed from steepest descent to conjugate gradient. A constant dielectric of $\varepsilon = 1$ was used.

The molecular dynamics simulations were performed with a starting temperature of 10 K followed by slowly heating to the reference temperature of 300 K at which the systems were to be kept. We applied the Berendsen algorithm for the coupling to an extend bath using a scaling factor of 0.2 ps [18]. After 2 ps the systems equilibrated at 300 K, the dynamics runs were carried out for 800 ps and the N, V, P ensemble was applied. The X-H bonds were constrained to constant values with the SHAKE procedure of AMBER. The time steps were 2 fs and the nonbonded list was updated after 25 fs.

The frequency of all dihedral angles particularly the dihedral angle Φ of all amino acid residues was graphically analyzed (see e.g. Figure 1) and compared with the experimental results based on Karplus equations. Those conformation with the highest average frequency in the simulation time that agreed with the dihedral angles Φ derived from the Karplus equations was used to generate a major solution conformation which was subsequently minimized in solution. The stability of the conformation was proved by a further dynamics simulations using the same conditions as described above without NMR distance restraints (see Figure 2).

The previously published model of the active site of DP IV [13] has been developed by us based on experimental data using force field calculations with the TRIPOS force field [19]. For our studies presented here this model was

Table 2 *Observed NOE cross peaks in ROESY spectra and calculated interproton distances (Å) obtained from the energy minimized solution structures*

		Tat(1–9) Xaa^5=Asp, Xaa^6=Pro		**L^6–Tat(1–9)** Xaa^5=Asp, Xaa^6=Leu		**I^5–Tat(1–9)** Xaa^5=Ile, Xaa^6=Pro	
		NOEs (obs.)	r(H,H) (calc.)	NOEs (obs.)	r(H,H) (calc.)	NOEs (obs.)	r(H,H) (calc.)
Asp^{2}N$^\alpha$H	Met^{1}C$^\alpha$H	st[a]	2.37	st	2.23	st	2.15
Asp^{2}N$^\alpha$H	Met^{1}C$^\beta$H	–	–	w	3.86	m	3.34
Asp^{2}N$^\alpha$H	Met^{1}C$^\gamma$H	w[c]	4.23	–	–	–	–
Asp^{2}C$^\alpha$H	Pro^{3}C$^\delta$H$_2$	st	2.45	–	–	–	–
Asp^{2}C$^\alpha$H	Pro^{3}C$^\delta$H$_A$	–	–	st	2.38	m	2.60
Asp^{2}C$^\alpha$H	Pro^{3}C$^\delta$H$_B$	–	–	st	2.49	m	2.20
Pro^{3}C$^\delta$H$_B$	Asp^{2}C$^\beta$H$_A$	–	–	–	–	w	4.45
Val^{4}N$^\alpha$H	Pro^{3}C$^\alpha$H	st	2.40	st	2.35	st	2.45
Xaa^{5}N$^\alpha$H	Val^{4}C$^\alpha$H	st	2.42	st	2.40	st	2.20
Xaa^{5}N$^\alpha$H	Val^{4}C$^\beta$H	w	2.34	w	2.40	–	–
Xaa^{5}N$^\alpha$H	Val^{4}C$^\gamma$H$_3$	w	4.16	w	4.32	–	–
Xaa^{5}C$^\alpha$H	Xaa^{6}C$^\delta$H$_2$	st	2.21	–	–	–	–
Xaa^{5}C$^\alpha$H	Xaa^{6}C$^\delta$H$_A$	–	–	–	–	m	2.30
Xaa^{5}C$^\alpha$H	Xaa^{6}C$^\delta$H$_B$	–	–	–	–	m	2.94
Xaa^{6}N$^\alpha$H	Xaa^{5}C$^\alpha$H	–	–	w	3.50	–	–
Asn^{7}N$^\alpha$H	Xaa^{6}C$^\alpha$H	st	2.36	st	2.37	st	2.41
Asn^{7}N$^\alpha$H	Xaa^{6}C$^\beta$H$_2$	–	–	m[b]	3.06	m	2.78
Asn^{7}N$^\alpha$H	Xaa^{6}C$^\gamma$H	–	–	w	3.87	–	–
Asn^{7}N$^\alpha$H	Ile^{8}N$^\alpha$H	–	–	w	4.37	w	4.48
Glu^{9}N$^\alpha$H	Ile^{8}C$^\alpha$H	st	2.39	st	2.46	st	2.15
Glu^{9}N$^\alpha$H	Ile^{8}C$^\beta$H	–	–	–	–	w	4.37
Glu^{9}N$^\alpha$H	Ile^{8}C$^\gamma$H$_3$	w	4.25	w	4.07	–	–
Glu^{9}N$^\alpha$H	Ile^{8}N$^\alpha$H	–	–	–	–	w	4.07

[a] st = strong; [b] m = middle; [c] w = weak

reoptimized in vacuum with the Amber 4.1 force field . No relevant alterations could be observed (RMSD=0.987 Å).

Several Tat / DP IV complexes were constructed manually on the basis of the solution conformations obtained by the molecular dynamics simulations. Starting with the formation of a strong salt bridge between the negatively charged side chain of Asp^{739} of the DP IV model and the protonated N-terminus, the inhibitor was anchored at this site and different orientations of the peptide chain within the binding pocket were chosen as starting structures for subsequent energy optimization. Energy optimizations of the enzyme ligand complexes were carried out with fixed Cα-atoms of the enzyme model as described earlier [13]. The interaction energies between the ligands and the enzyme model were estimated by subtracting the energy of the individual components from the energy optimized structure of the formed complex.

Moreover, docking of the solution conformations of the Tat peptides was also carried out using the program FLEXIDOCK included in SYBYL [20]. However, the model of the active site of DP IV is to small to obtain relevant results. This program tries to find also interactions of the three C-terminal amino acid residues of the Tat peptides and creates energetically unfavorable conformations.

Molecular dynamics simulations were also performed of the P^2-Tat(1-9) derivative. Since, there are no NMR data available these simulations were performed without distance restraints. Taking into account the dihedral angle Φ of Asp^2 of about –70° (see Table 1) the proline residue in position 2 can adopt a similar backbone structure because in the pyrrolidine ring this angle is fixed close to this value.

All figures were prepared with the molecular modeling program SYBYL 6.3 on Silicon Graphics workstations [20].

^{1}H NMR spectroscopy

^{1}H NMR spectra in H_2O/D_2O were measured at 303 K at 6 mM peptide concentration and pH=4 on Bruker ARX500 and Varian UNITY 500 spectrometers. Chemical shifts were calibrated with respect to 3-(trimethylsilyl)-3,3,2,2-tetradeutero-

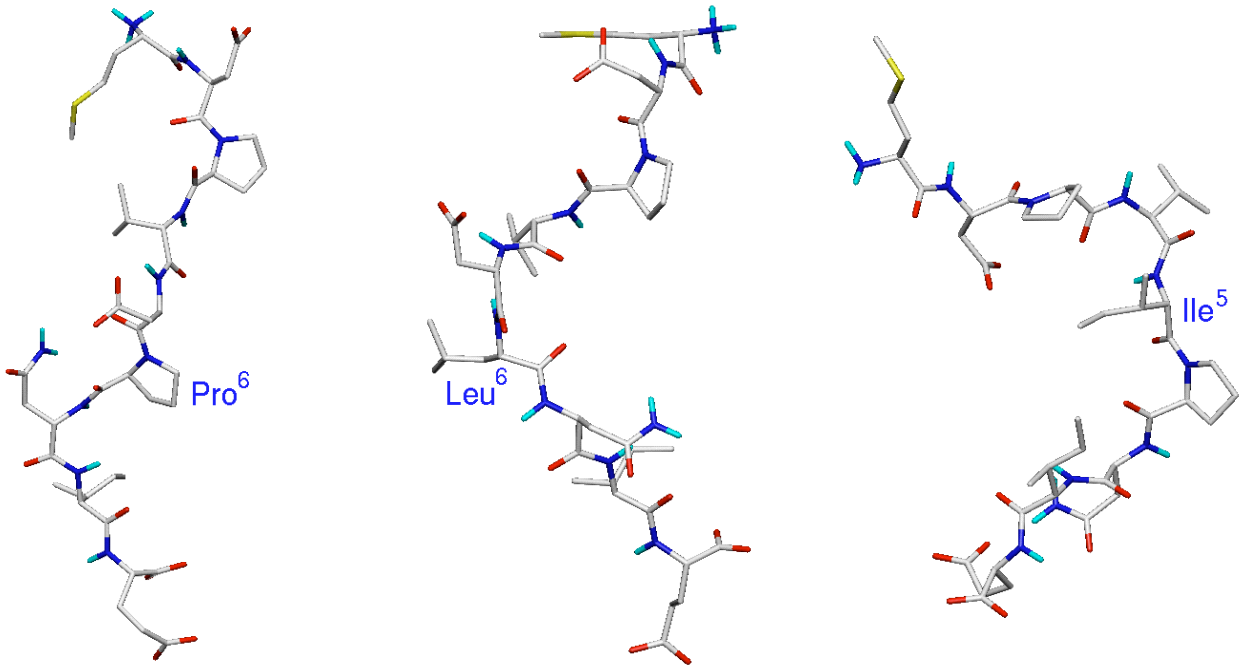

Figure 3 *Representation of the determined solution conformations of a) Tat(1-9), b) L⁶-Tat(1-9) and c) I⁵-Tat(1-9)*

propionic acid (sodium salt). Torsion angles Φ were calculated using Karplus-type equations. ROESY spectra (mixing time, t_m = 300 ms) were recorded in the phase-sensitive mode using the TPPI or States-Haberkorn-Ruben methods. For ROESY, 512 FIDs of 2K data points, 24 scans each, were acquired. In both dimensions, the data were processed using π/2 shifted squared sinebell weighting functions. Zerofilling to 2K was applied in ω_1.

Results

The solution conformations of Tat(1-9) and its derivatives

The solution conformations were determined on the basis of the experimental data listed in Tables 1 and 2. The RMSD residual distance violations of Tat(1-9), L⁶-Tat(1-9) and I⁵-Tat(1-9) relative to the experimental restraints were on average 0.22, 0.27 and 0.26 Å, respectively.

Analysis of the dynamics trajectories of the dihedral angles Φ, Ψ and χ_1 in the distance restraints simulations gives insight into the conformational flexibility and different conformational behavior of all three peptides and was the basis for the determination of the major solution conformations. In Figure 1 conformational maps of the torsion angles Φ and Ψ of the amino acid residues four, five and six of the three nonapeptides are represented for comparison.

The amide proton of Asp⁵ of the native Tat forms alternate intramolecular hydrogen bonds to the own side chain, partially to the side chain of Asn⁷ and intermolecular hydrogen bonds to the solvent molecules. These fluctuations of the hydrogen bonds are accompanied by a relatively high flexibility of the torsion angle Φ of Asp⁵ (Figure 1a). Asn⁷N$^{\alpha}$H of Tat(1-9) forms intramolecular hydrogen bonds to the carboxyl oxygen of Asp⁵ and its own side chain and not to the solvent. For this reason, the fluctuations of the torsion angle Φ of Asn⁷ are relatively low.

The exchange of the relatively inflexible Pro⁶ by Leu causes an increase of the flexibility of Φ and Ψ for this residue in L⁶-Tat(1-9) and also of the residues five and seven in comparison to the native peptide (Figure 1). Substantial stronger fluctuations of the L⁶-Tat(1-9) derivative compared to the native nonapeptide were found for the torsion angle Ψ of Asp⁵ (see Figure 1b). For this derivative the tendency to form hydrogen bonds between Asp⁵NH and the own side chain is clearly reduced. The hydrogen bonds often change between Asp⁵NH and Asp⁵CO and the side chain of Asn⁷.

In the case of the I⁵-Tat(1-9) peptide the bulky and unpolar side chain of Ile⁵ is not able to enter into hydrogen bonds. The substitution of Asp⁵ by Ile leads to a restriction of the conformational flexibility around this residue but increases the flexibility of Asn⁷ (Figure 1c).

The major solution conformations of Tat(1-9), I⁵-Tat(1-9) and L⁶-Tat(1-9) were derived by taking into account dihedral angles Φ resulting from Karplus equations and by considering their frequency of occurrence in the molecular dynamics simulations (see Table 1 and Figure 3). In this way, energy minimized conformations in solution reasonably well reproduce the characteristic features of the experimental observations derived from ^{1}H NMR measurements for all three pep-

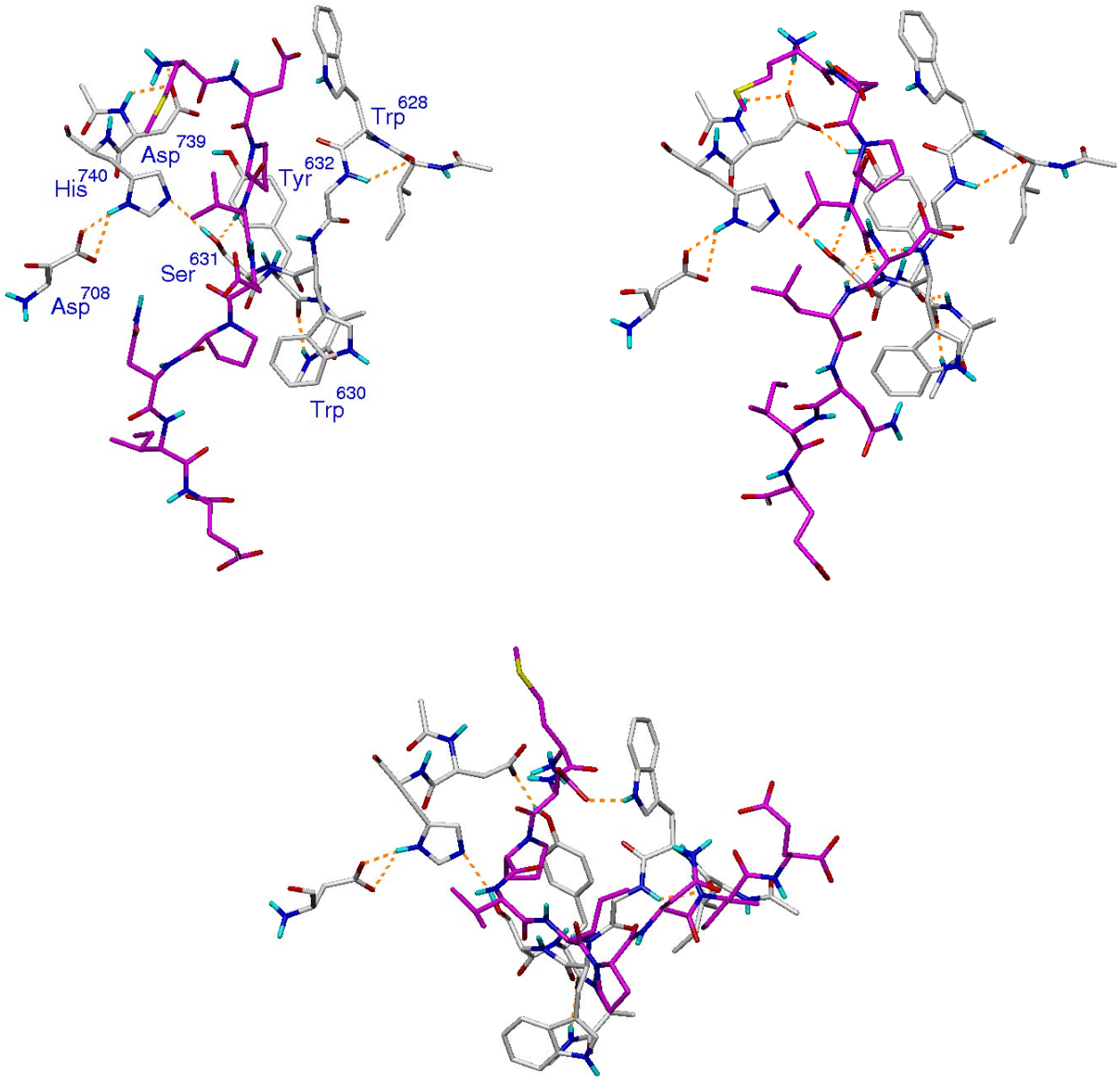

Figure 4 *Representation of the docking of a) Tat(1-9), b) L*^{6}*-Tat(1-9) and c) I*^{5}*-Tat(1-9) into the binding pocket of the model of the active site of DP IV. The Tat derivatives are colored magenta*

tides (see Tabs. 1 and 2). The comparison of measured distances and experimental NOEs obtained from 2D NMR ROESY spectra is shown in Table 2. Most of the distances of the solution conformations are in agreement with the NOEs. One exception is the weak NOE between the $C^{\beta}H$ proton of Val^4 and the amide proton of Asp^5 in Tat(1-9) and L^6-Tat(1-9) but the calculated distances (2.34 Å or 2.40 Å, respectively) should indicate a strong NOE. We tried to change the value for the torsion angle χ_1 of Val^4 for a weak NOE. However, after optimizing a short distance resulted between the $C^{\gamma}H$ of Val^4 and Asp^{5}NH which is in contradiction to the experimental results. Moreover, the conformation with a close distance between Val$^4C^{\beta}H$ and Asp^{5}NH was energetically preferred over the other conformation. Therefore, we excluded the modified conformation in further investigations. Probably, there is a high conformational flexibility around the side chain of Val^4 leading to weak NOEs.

The solution conformations defined on the basis of experimental results should now be compared to each other in detail. The exchange of Pro^6 with Leu leads to a change of the torsion angles Φ of Val^4 and Ψ of Asp^5 and Asn^7 (Figure 3b, Table 1). In the parent Tat(1-9) the strong NOE between

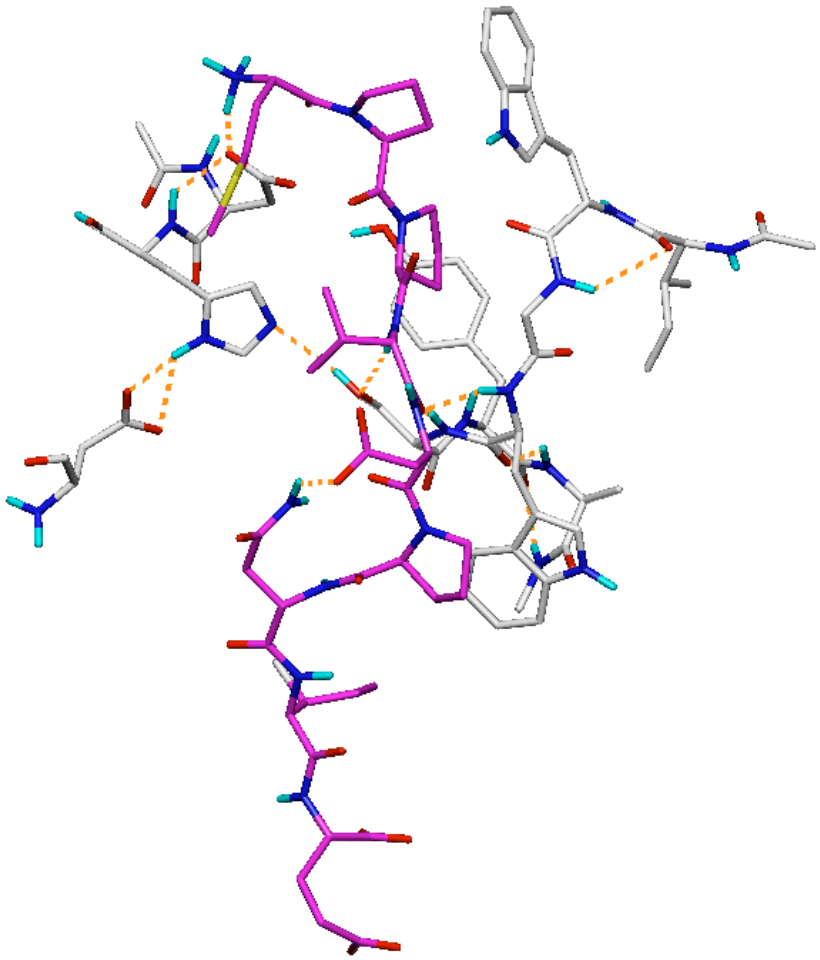

Figure 5 *Representation of the docking of P²-Tat(1-9) (magenta) into the model of the active site of DP IV*

the $C^{\alpha}H$ proton of Asp^5 and the $C^{\delta}H$ protons of Pro^6 indicates a torsion angle Ψ of about 160°. However, in L^6-Tat(1-9) only a weak NOE between the $C^{\alpha}H$ proton of Asp^5 and the amide proton of Leu^6 occurs thus resulting in a torsion angle Ψ of Asp^5 of -20°.

The alteration of the torsion angle Ψ of Asn^7 in Tat(1-9) from 42° to 155° in L^6-Tat(1-9) was also confirmed by the 2D NMR data. In the ROESY spectrum of L^6-Tat(1-9) a weak NOE was observed between the amide protons of Asn^7 ($N^{\alpha}H$) and Ile^8 which was not found for Tat(1-9) (Table 2). The other dihedral angles are in agreement with those of Tat(1-9).

In the case of I^5-Tat(1-9) stronger conformational differences in the peptide chain of the determined solution conformation were observed compared to the native Tat(1-9) and L^6-Tat(1-9).

The torsion angles Φ of Asp^2, Val^4, Ile^5, Asn^7 and Glu^9 as well as the torsion angles Ψ of Asp^2, Val^4, Asn^7 and Ile^8 are very different from those of the other two Tat peptides (Table 1). These strong alterations of the backbone of I^5-Tat(1-9) are apparent from the experimental NOEs of the ROESY spectrum of this peptide (Table 2).

The strong NOEs in the native Tat(1-9) between the $C^{\alpha}H$ proton of Asp^2 and the $C^{\delta}H$ protons of Pro^3 were weakened to middle NOEs through the rotation of Φ of Asp^2 from -70° in Tat(1-9) to -139° in I^5-Tat(1-9). Furthermore, an additional NOE was observed between the $C^{\beta}H$ proton of Asp^2 and $Pro^3C^{\delta}H$. NOEs between the $C^{\gamma}H$ protons of Met^1 and the amide proton of Asp^2 were not found. Instead, NOEs between $Met^1C^{\beta}H$, $Met^1C^{\alpha}H$ and $Asp^2N^{\alpha}H$ were obtained.

The change in the backbone angle Φ of Asp^5 in Tat(1-9) from -66° to -139° of Φ of Ile^5 in I^5-Tat(1-9) causes the reduction of NOE intensity in the ROESY spectrum of this Tat derivative between the $C^{\alpha}H$ proton of Ile^5 and the $C^{\delta}H$ protons of Pro^6. In contrast, in the native Tat(1-9) the NOE between $Asp^5C^{\alpha}H$ and $Pro^6C^{\delta}H_2$ is strong.

Due to the change of the torsion angle Φ of Asn^7 from -138° in Tat(1-9) to -64° in I^5-Tat(1-9) additional weak NOEs were obtained between the amide protons of Asn^7 and Ile^8 as well as between $C^{\beta}H$ of Pro^6 and $Asn^7N^{\alpha}H$ in the I^5 analogue.

Moreover, the rotation of Φ of Glu^9 from -86° to -138° leads to a loss of the NOE between $Ile^8C^{\gamma}H$ and Glu^9NH of I^5-Tat(1-9). Now a new NOE between the amide protons of Ile^8 and Glu^9 (Table 2) appears.

The change of several dihedral angles Ψ in I^5-Tat(1-9) in comparison to Tat(1-9) and L^6-Tat(1-9) is also indicated by

observed NOEs which are weakened or not obtained in I^5-Tat(1-9) and by the occurrence of new NOEs (Table 2).

Docking of the Tat peptide solution conformations into the model of the active site of DP IV

The obtained solution conformation of the native Tat(1-9) was manually docked into the model of the active site of DP IV (Figure 4a) (*see Methods Section*). As shown in Figures 3 and 4 the lowest energy structure of Tat(1-9) in the binding pocket agrees well with the solution conformation. The RMSD between the main chain atoms of the Tat peptides bound and free are 0.7223 Å of Tat(1-9), 1.559 Å of L^6-Tat(1-9), and 0.895 Å of I^5-Tat(1-9).

Several attractive interactions of Tat(1-9) with the active site of DP IV can be detected. The positively charged N-terminus of Met^1 is recognized by the side chain of Asp^{739}. Hydrophobic interactions occur between the pyrrolidine ring of Pro^3 with Tyr^{632} of the active site of DP IV. In this way, Pro^3 assumes a position like proline in substrates of DP IV. However, the dihedral angle Ψ_3 in Tat(1-9) adopts a value of 160° whereas in substrates this angle has to be about 80° [12]. For this reason, an attack of the active serine to the carbonyl carbon atom of the peptide bond between Pro^3 and Val^4 is impossible. This explains the behavior of the Tat(1-9) peptides as competitive inhibitors. An additional attractive hydrophobic interaction occurs between the pyrrolidine ring of Pro^6 and the side chain of Trp^{630}. Hydrogen bonds are formed between the carbonyl oxygen of Val^4 and the amide proton of Trp^{630} and Ser^{631} as well as between Val^4NH and the hydroxyl oxygen of the side chain of Ser^{631}. The estimated interaction energy of Tat(1-9) with the model is -53.7 kcal·mol^{-1}.

Since we did not consider solvation and dissolvation effects as well as entropy contributions in the docking procedure the calculated interaction energy represents only an estimation of the free interaction energy.

The three compounds are highly similar to each other in the sequence modified just by one amino acid residue these contributions might be similar in first approach. Therefore, comparing all three complexes a smaller (more negative) interaction energy should correlate with higher affinity of the Tat derivative to the active site of DP IV and consequently with a higher inhibitory potency.

The used model of DP IV has been developed on the basis of published site directed mutagenesis studies of amino acid residues of the active site of DP IV. There are no more experimental results available that could help to enlarge the model in an appropriate manner. Therefore, the model of the active site of DP IV is relatively small and no conclusion with respect to interactions of the C-terminal amino acid residues 7 to 9 of Tat(1-9) can be drawn. We cannot yet decide how the remaining three amino acid residues influence the inhibitory activity. It might be that the remaining three C-terminal amino acid residues have low affinity to the active site of DP IV. Moreover, most of the known DP IV specific inhibitors represent di- and tripeptides for which the correlation between their interaction energies with the active site model of DP IV and the experimental pK_i values have been shown [13]. It might be assumed that the formed attractive interactions of the first six amino acid residues are mainly responsible for the high affinity and inhibitory activity of Tat(1-9) to DP IV.

In the case of L^6-Tat(1-9) the formation of a salt bridge between the positively charged N-terminus of Met^1 and the negatively charged side chain of Asp^{739} is also possible. Furthermore, similar hydrogen bonds can be detected compared to the Tat(1-9). The amide proton of Val^4 and the negatively charged side chain of Asp^5 form hydrogen bonds to the amino acid residues of the active site of DP IV. The side chain of Asp^5 can form a weak intermolecular hydrogen bond to the amide proton of Trp^{630} in contrast to the native Tat(1-9).

However, not all attractive interactions of the native Tat(1-9) are possible in the case of the L^6-Tat(1-9) derivative (Figure 4b). As mentioned above, for the native Tat(1-9) an attractive hydrophobic interaction between Pro^6 and Trp^{630} occurred. In the case of L^6-Tat(1-9) the solution conformation is different from that of the parent peptide at this residue, the side chain of the substituted Leu^6 shows in a direction where we have no information about the structure of DP IV. We cannot exclude that spatial repulsion with any other amino acid close to the active site of DP IV will occur in this area. As ever it is, the hydrophobic interaction in this position is lost. This seems to be the main reason for the reduced interaction energy (-50.2 kcal·mol^{-1}) with DP IV in comparison to the native Tat(1-9).

Taking into account that in an induced fit mechanism the L^6-Tat(1-9) derivative may adopt a conformation which is similar to that one of Tat(1-9) in the docked solution conformation, Pro^6 was substituted with Leu. In this case, the bulky side chain of Leu^6 causes spatial hindrance with the side chain of Trp^{630}. An energy optimization of this structure forces the L^6-Tat(1-9) considerably out of the binding pocket. This led to a conformation of L^6-Tat(1-9) where the Leu^6 residue could perform attractive interactions with Trp^{630} but simultaneously other interactions were weakened particularly those of Pro^3 and Val^4 including the hydrogen bonds of these residues to the model. These results are also expressed by the considerably reduced interaction energy (-21.2 kcal·mol^{-1}).

Since in either case the interaction energy of L^6-Tat(1-9) is reduced in comparison to the native compound the low inhibitory activity can now be explained.

The solution conformation of I^5-Tat(1-9) assumes a different orientation in the binding pocket characterized by fewer attractive interactions. It is therefore not surprising that in contrast to both Tat(1-9) and L^6-Tat(1-9) a number of attractive interactions to the active site model of DP IV are no longer possible (Figure 4c). This is in agreement with the low competitive inhibitory activity. The salt bridge between the charged N-terminus of I^5-Tat(1-9) and Asp^{739} of DP IV can be formed whereas the two important hydrophobic interactions of Pro^3 with the side chain of Tyr^{632} and of Pro^6 with Trp^{630} are nearly completely removed in comparison to the native nonapeptide. This is also caused by a considerably different conformation at Ile^5 which leads to spatial hindrance

between the side chain of this residue and Gly^{629} of the active site of DP IV. This repulsion prevents the diving of this derivative into the binding pocket of DP IV.

The calculated interaction energy between I^5-Tat(1-9) and DP IV is about 15 kcal·mol^{-1} lower (-38.2 kcal·mol^{-1}) in comparison to the native Tat(1-9). No other complexes with lower interaction energy considering different conformations of the ligand as well as modified orientations to the enzyme model were found.

Discussion

The determined solution conformations of the three nonapeptides show some differences. These conformational alterations caused by the substitutions in positions five and six are very likely responsible for the reduced inhibitory strength of these derivatives but it could not be excluded that the bulkiness of the side chains of Ile and Leu per se prevents effective binding to DP IV.

Though the model of DP IV is relatively small the molecular modeling results in combination with experimental data obtained from NMR spectroscopy are strong indications that the N-terminal part of Tat binds into the active site of DP IV.

The estimated interaction energies of all three Tat derivatives (Tat(1-9) -53.7 kcal·mol^{-1}, L^6-Tat(1-9) -50.2 kcal·mol^{-1} and I^5-Tat(1-9) -38.2 kcal·mol^{-1}) are in the same sequence like the inibitory potency (60%, 20%, 10%). Although we have no experimental indications the modeling investigations suggest that the docking conformations of the Tat peptides to DP IV are similar to their solution conformations except small conformational alterations. Taking into account that the interactions of the Tat peptides with the model of the active site of DP IV include only the first six residues of the Tat derivatives we cannot yet decide how the remaining three amino acid residues influence the inhibitory activity. It might be that the remaining three C-terminal amino acid residues have low affinity to the active site of DP IV. A series of hexapeptides not derived from Tat but also with a proline residue in the third position have been tested with regard to their inhibitory potency [8]. These compounds show also up to 20 % inhibition of the DP IV catalyzed hydrolysis. Therefore, the theoretical results described here suggest that the first six amino acid residues mainly contribute to the interaction energies of the Tat derivatives with DP IV. However, as a result of the theoretical investigations presented in this paper it can be concluded that the synthesis and testing of inhibitory potencies of hexapeptides particularly of the native Tat sequence should be the subject of future studies.

From the modeling investigations some conclusions concerning the importance of single amino acid residues of Tat(1-9) for their interaction with DP IV can be drawn.

The N-terminal methionine forms an important salt bridge with Asp^{739}. However, we have no indications for interactions of the side chain of this residue with DP IV. Therefore, the synthesis of Tat(1-9) derivatives with substitution of Met^1 by any other unprotected amino acid residue will give more insight to this question.

Interestingly, the substitution of Asp^2 by Pro leads to a slightly enhanced inhibitory potency in comparison to Tat(1-9). NMR investigations of this compound have not yet been performed. The conformation of P^2-Tat(1-9) docked into the model of the active site of DP IV forms hydrophobic interactions between Pro^2 and Trp^{628} stabilizing the enzyme ligand complex (Figure 5). The estimated interaction energy is –53.0 kcal·mol^{-1} similar to those of the native peptide. In agreement with our model this indicates that the nature of the amino acid residue in position 2 is of high importance for the interaction with DP IV.

The proline at the third position exhibits hydrophobic interactions with Tyr^{632}. Since we assume that this type of interaction might be the same as for substrate peptides with proline or alanine in position 2, it can be predicted that proline in position 3 can be substituted by alanine, but not by any other amino acid residue, without considerable loss of inhibitory strength. For valine at the fourth position we have no clear information on its influence to the inhibitory action.

The exchange of the negatively charged Asp^5 by the hydrophobic Ile and the missing hydrogen bonds between the negatively charged side chain of Asp^5 and the DP IV model decrease the inhibitory activity. The bulky side chain of Ile has a strong obstructive effect. For this reason Asp at the fifth position is essential. This argument is also valid for the proline in the sixth position because of its hydrophobic interactions to Trp^{630}.

Summarizing, it can be concluded that the results of the conformational investigations on the three Tat derivatives based on NMR investigations and molecular dynamics simulations give an idea of the interactions of Tat(1-9) nonapeptide sequences with DP IV explaining the biological results. The assumption that the N-terminal sequence of HIV-1 Tat as competitive inhibitor interacts directly with the active site of DP IV could be confirmed by the present study.

Acknowledgements We are grateful for research support from the Ministerium für Wissenschaft und Forschung von Sachsen-Anhalt (Grant 1185A/0083) and by Deutsche Forschungsgemeinschaft (SFB 387 / TP A8).

References

1. Lane, H.C.; Depper, J.M.; Greene, W. C.; Whalen, G.; Wahlmann, T.A.; Fauci, A.S. *N. Engl. J. Med.* **1985**,*313*, 79.
2. Helland, D.E.; Welles, J.L.; Caputo, A.; Haseltine, W.A. *J. Virol* **1991**, *65*, 4547.
3. Viscidi, R.P.; Mayur, K.; Lederman, H.M.; Frankel, A.D. *Science* **1989**, *246*, 1606.
4. Fauci, A.S., Science **1988**, *239*, 617.
5. Gutheil, W.G.; Subramanyam, M.; Flentke, G.R.; Sanford, E.M.; Huber, B.T.; Bachovchin, W.W. *Proc. Natl. Acad. Sci., USA* **1994**, *91*, 6594.

6. Reinhold, D.; Wrenger, S.; Bank, U.; Bühling, F.; Hoffmann, T.; Neubert, K.; Kraft, M.; Frank, R.; Ansorge, S. *Immunobiology* **1996**, *195*, 119.
7. Schmitz, T.; Underwood, R.; Khiroya, R.; Bachovchin; W.W.; Huber, B.T. *J. Clin. Invest.* **1996**, *97*, 1545.
8. Wrenger, S.; Reinhold, D.; Hoffmann, T.; Kraft, M.; Frank, R.; Faust, J.; Neubert, K.; Ansorge, S. *FEBS Letters* **1996**, *383*, 145.
9. Wrenger, S.; Hoffmann, T.; Faust, J.; Mrestani-Klaus, C.; Brandt, W.; Neubert, K.; Kraft, M.; Olek, S.; Frank, R.; Ansorge, S.; Reinhold, D. *J. Biol. Chem.* **1997**, *272 (48)*, 30283.
10. Heins, J.; Neubert, K.; Barth, A.; Canizaro, P.C.; Behal F. *J. Biochim. Biophys. Acta* **1984**, *785*, 30.
11. Fischer, G.; Heins, J.; Barth, A. *Biochim. Biophys. Acta* **1983**, *742*, 452.
12. Brandt, W.; Lehmann, T.; Hoffmann, T.; Schowen, R.L.; Barth, A. *J. Comput.-Aided Mol. Des.* **1992**, *6*, 159.
13. Brandt, W.; Lehmann, T.; Thondorf, I.; Born, I.; Schutkowski, M.; Rahfeld, J.-U.; Neubert, K.; Barth, A. *Int. J. Peptide Protein Res.* **1995**, *46*, 494.
14. Brandt, W.; Ludwig, O.; Thondorf, I.; Barth, A. *Eur. J. Biochem.* **1996**, *236*, 109.
15. Mrestani-Klaus, C.; Fengler, A.; Brandt, W.; Faust, J.; Wrenger, S.; Reinhold, D.; Ansorge, S.; Neubert, K. *J. Pept. Sci*, submitted.
16. Weiner, S.J.; Kollmann, P.A.; Case, D.A.; Singh, U.C.; Ghio, C.; Alagano, G.; Profeta, Jr., S.; Weiner, P. *J. Am. Chem. Soc.* **1984**, *106*, 765.
17. Weiner, S.J.; Kollmann, P.A.; Nguyen, D.T.; Case, D.A. *J. Comput. Chem.* **1986**, *7*, 230.
18. Berendsen, H.J.C.; Postma, J.P.M.; van Gunsteren, W.F.; DiNola, A.; Haak, J.R. *J. Chem. Phys.* **1984**, *81*, 3684.
19. Clark,M.; Cramer III, R.D.; van Opdenbosch, N. *J. Comp. Chem.* **1989**, *10*, 982.
20. TRIPOS Associates, Inc., 1699 S. Hanley Road, St. Louis, Missouri 63144-2913, 1996